Author Manuscript

Author Manuscript

Author Manuscript

Author Manuscript

HHS Public Access

Author manuscript

J Autoimmun. Author manuscript; available in PMC 2016 September 01.

Published in final edited form as:

J Autoimmun. 2015 September ; 63: 76–87. doi:10.1016/j.jaut.2015.07.010.

Treatment of Cholestatic Fibrosis by Altering Gene Expression of Cthrc1: Implications for Autoimmune and non-Autoimmune Liver Disease

Zhaolian Bian[a,*], **Qi Miao**[a,*], **Wei Zhong**[a,*], **Haiyan Zhang**[a], **Qixia Wang**[a], **Yanshen Peng**[a], **Xiaoyu Chen**[a], **Canjie Guo**[a], **Li Shen**[a], **Fan Yang**[a], **Jie Xu**[a], **Dekai Qiu**[a], **Jingyuan Fang**[a], **Scott Friedman**[b], **Ruqi Tang**[a], **M. Eric Gershwin**[c], and **Xiong Ma**[a]

Zhaolian Bian: bianzhaolian1998@163.com; Qi Miao: miaoqi0730@126.com; Wei Zhong: rjzhongwei@163.com; Haiyan Zhang: heidi0509@163.com; Qixia Wang: wqx0221155@126.com; Yanshen Peng: pengyanshen@yahoo.com.cn; Xiaoyu Chen: 1621508481@qq.com; Canjie Guo: guocanjie@yahoo.com.cn; Li Shen: shirleypear@126.com; Fan Yang: flyingfish_yf@163.com; Jie Xu: jiexu@yahoo.com; Dekai Qiu: qiudekai2008@126.com; Jingyuan Fang: fangjingyuan_new@163.com; Scott Friedman: scott.friedman@mssm.edu; Ruqi Tang: ruqi.tang@gmail.com; M. Eric Gershwin: megershwin@ucdavis.edu; Xiong Ma: maxiongmd@hotmail.com

[a]State Key Laboratory for Oncogenes and Related Genes, Key Laboratory of Gastroenterology & Hepatology, Ministry of Health, Division of Gastroenterology and Hepatology, Ren Ji Hospital, School of Medicine, Shanghai Jiao Tong University, Shanghai Cancer Institute, Shanghai Institute of Digestive Disease, 145 Middle Shandong Road, Shanghai 200001, China

[b]Division of Liver Diseases, Icahn School of Medicine at Mount Sinai, New York, USA

[c]Division of Rheumatology, Allergy, and Clinical Immunology, University of California at Davis, Davis, CA, USA

Abstract

Collagen triple helix repeat containing-1 (Cthrc1) is a documented specific inhibitor of TGF-β signaling. Based on this observation, we developed the hypothesis that knocking in/knocking out the Cthrc1 gene in murine models of cholestasis would alter the natural history of cholestatic fibrosis. To study this thesis, we studied two murine models of fibrosis, first, common bile duct ligation (CBDL) and second, feeding of 3, 5-diethoxy-carbonyl-1, 4-dihydrocollidine (DDC). In both models, we administered well-defined adenoviral vectors that expressed either Cthrc1 or, alternatively, a short hairpin RNA (shRNA)-targeting Cthrc1 either before or after establishment of fibrosis. Importantly, when Cthrc1 gene expression was enhanced, we noted a significant improvement of hepatic fibrosis, both microscopically and by analysis of fibrotic gene expression. In contrast, when Cthrc1 gene expression was deleted, there was a significant exacerbation of

Please address correspondence to: Xiong Ma, & Ruqi Tang, State Key Laboratory for Oncogenes and Related Genes, Key Laboratory of Gastroenterology & Hepatology, Ministry of Health, Division of Gastroenterology and Hepatology, Ren Ji Hospital, School of Medicine, Shanghai Jiao Tong University, Shanghai Cancer Institute, Shanghai Institute of Digestive Disease, 145 Middle Shandong Road, Shanghai 200001, China, 200001. Tel: 86-21-63200874, Fax: 86-21-63266027, maxiongmd@hotmail.com, ruqi_tang@126.com. OR M. Eric Gershwin, M.D., Division of Rheumatology, Allergy and Clinical Immunology, University of California at Davis School of Medicine, Genome and Biomedical Sciences Facility, 451 Health Sciences Drive, Suite 6510, Davis, CA 95616; Telephone: 530-752-2884; Fax: 530-752-4669; megershwin@ucdavis.edu.

*These authors contributed equally to this paper.

Publisher's Disclaimer: This is a PDF file of an unedited manuscript that has been accepted for publication. As a service to our customers we are providing this early version of the manuscript. The manuscript will undergo copyediting, typesetting, and review of the resulting proof before it is published in its final citable form. Please note that during the production process errors may be discovered which could affect the content, and all legal disclaimers that apply to the journal pertain.

Author Manuscript Author Manuscript Author Manuscript Author Manuscript

fibrosis. To identify the mechanism of action of these significant effects produced by knocking in/knocking out Cthrc gene expression, we thence studied the interaction of Cthrc1 gene expression using hepatic stellate cells (HSCs) and human LX-2 cells. Importantly, we demonstrate that Cthrc1 is induced by TGF-β1 via phospho-Smad3 binding to the promoter with subsequent transcription activation. In addition, we demonstrate that Cthrc1 inhibits TGF-β signaling by accelerating degradation of phospho-Smad3 through a proteosomal pathway. Importantly, the anti-fibrotic effects can be recapitulated with a truncated fragment of Cthrc1. In conclusion, our findings uncover a critical negative feedback regulatory loop in which TGF-β1 induces Cthrc1, which can attenuate fibrosis by accelerating degradation of phospho-Smad3.

hepatic fibrosis; cholestatic liver fibrosis; hepatic stellate cell; anti-fibrotic treatment; TGF-β pathway

2.1 Introduction

Hepatic fibrosis develops in most chronic liver diseases, including viral hepatitis, cholestasis, alcohol consumption, autoimmune and non-alcoholic fatty liver diseases, and is characterized by excessive accumulation of extracellular matrix (ECM) [1–5]. Hepatic stellate cells (HSCs), a non-parenchymal cell population in the liver, are considered the most relevant sources of ECM and the TGF-β 1/Smad3 pathway is the most potent profibrogenic factor involved in initiation and maintenance of such fibrogenesis [6]. Indeed, strategies that block TGF-β 1/Smad3 have a significant anti-fibrotic effect in animal models [7–10], but testing of these therapies in human liver fibrosis has been disappointing with limited efficacy [11] and often accompanied by adverse events [12].

The collagen triple helix repeat containing-1 (Cthrc1) is a highly conserved protein; human Cthrc1 shares 92% sequence identity with the rat homolog [13] and was initially discovered in a screen for differentially expressed genes in a rat model of balloon-injured vasculature [14]. Repression of TGF-β signaling was observed in Cthrc1 transgenic mice, with reduced phospho-Smad2/3 levels in smooth muscle but not endothelial cells [15]. We therefore postulated that Cthrc1 had the potential to modulate hepatic fibrogenesis. To explore this issue, we studied two murine models of liver fibrosis, common bile duct ligation (CBDL) and exposure to 3, 5-diethoxycarbonyl-1, 4-dihydrocolidine (DDC). We report that enhancement Cthrc1 gene expression significantly alleviates both the induction of fibrosis and enhances its reversibility in established fibrosis. Further, through extensive *in vitro* molecule modeling, we demonstrate that these therapeutic effects occur by accelerating the degradation of phospho-Smad3. We suggest that use of Cthrc1 could have therapeutic potential to modulate cholestatic liver fibrosis by enhancing a critical and novel physiological negative feedback loop.

3.1 Methods

3.1.1 Murine models of fibrosis

We employed two well established models of murine fibrosis, common bile duct ligation (CBDL) or administration of 3, 5-diethoxycarbonyl-1, 4-dihydrocollidine (DDC). In CBDL,

Author Manuscript Author Manuscript Author Manuscript Author Manuscript

male C57BL/6 mice were anesthetized with 3.5% chloral hydrate (10ml/kg) and the common bile duct ligated twice with 6-0 silk sutures; for the purpose of control, a sham anesthetized operated group was included, but without bile duct ligation. In the second model, groups of C57BL/6 male mice at 6–8 weeks of age were fed a normal mouse diet supplemented with or without 0.1% DDC (Sigma Aldrich, St. Louis, MO) for periods of either 2 or 3.5 weeks. In both models we quantitated levels of Cthrc1 before and 5 days after CBDL and before and 14 days after DDC by immunohistochemistry, qPCR and immunoblot (n=5 in each group). Second, we transfected with an adenovirus vector expressing either the human Cthrc1 CDS region or a control (containing green fluorescent protein gene, GFP). Alternatively, we transfected with a short hairpin RNA (shRNA) targeting murine Cthrc1 or a control. In the CBDL model, the adenovirus vectors were injected either 3 days before or 3 days after the surgery and mice studied on day 5 (n=37), day 11 (n=25), and livers collected for analysis. In the DDC model, adenovirus vectors were injected 3 days before or 1 week after initiation of feeding; mice were studied at week 2 (n=27) or week 3.5 (n=30). The experimental outline, including induction and attenuation of fibrosis, is illustrated in Supplemental Figure 1. All animal experiments were approved by the Institutional Animal Care and Use Committee of School of Medicine, Shanghai Jiao Tong University. Liver tissues were processed for immunohistochemistry for detection of Cthrc1 [16] using antibody specific for Cthrc1 (Santa Cruz Biotechnology, Dallas, TX).

3.1.2 Cthrc1 and shRNA-expressing adenoviral vectors

The adenovirus (Ad) vectors Ad-Cthrc1, containing the human Cthrc1 CDS region or Ad-shCthrc1, containing an shRNA targeting the murine Cthrc1 mRNA, were expressed under a mCMV promoter [17]. The shRNA sequence was: 5'-GGAAGCCCTGAGTTAAATT-3'. The control adenovirus Ad-GFP or Ad-shGFP, was prepared in parallel. Recombinant adenoviruses were purified by velocity density gradient centrifugation in caesium chloride solutions. The infectious titer of recombinant adenoviruses were measured by plaque formation. A single dose of 2×10^9 plaque forming unit (PFU) of adenovirus was injected via the tail vein.

3.1.3 Mechanism of action of the Cthrc1 gene and modulation of fibrosis

Primary rat hepatic stellate cells (HSCs) from male Wistar rats (10–12 weeks of age) were cultured in DMEM medium (Invitrogen, Carlsbad, CA) with 10% fetal bovine serum (FBS, Invitrogen, v/v), 100 units/ml penicillin, and 100μg/ml streptomycin (Invitrogen) [1, 18, 19]. Viability was confirmed by trypan blue staining and was greater than 95%. HSCs were activated via cell culture on uncoated culture dishes for 7 days *in vitro* [18]. Cells were collected for qPCR, immunoblot, immunofluorescence and immunoprecipitation. The flow chart for this phase is shown in supplemental Figure 2A. For cell preparation and immunofluorescence, the cells were fixed with 4% paraformaldehyde, incubated with antibodies to Cthrc1, phospho-Smad3 (Santa Cruz Biotechnology) and finally imaged by confocal microscopy.

In a parallel experiment, human LX-2 cells were maintained at 37°C in an atmosphere of 5% carbon dioxide in Roswell Park Memorial Institute DMEM medium (Invitrogen) supplemented with 10% FBS, 100 units/ml penicillin, and 100 μg/ml streptomycin

Author Manuscript Author Manuscript Author Manuscript Author Manuscript

(Invitrogen). Before administration of TGF-β1 or PDGF-BB, LX-2 cells were starved for 16 hours, then immunoblotted for Cthrc1 (Supplemental Figure 2B). LX-2 cells were transfected with/without Ad-GFP or Ad-Cthrc1, and starved for 16 hours, then treated with TGF-β1 (5ng/ml) for 24 hours, finally profibrogenic genes was analyzed by quantitative real-time PCR(qPCR) (Supplemental Figure 2C). LY2109761 (10μM, Selleckchem, Houston, TX) or SB431542 (10μM, Selleckchem) were added 0.5 hour before the administration of TGF-β1(5ng/ml). MG-132 (30μM, Selleckchem) and SB431542 (10μM) were added when the TGF-β1 was washed out. The full length of Cthrc1 gene CDS or its truncations were inserted into the vector of pCDNA3.1. Plasmids or small interfering RNA (siRNA, GenePharma, Shanghai, China) were transfected by Lipofectamine 2000 (Invitrogen). The sequences of Cthrc1 siRNAs used in cell transfection were: 1) 5'-AAGCAGUGUUCAUGGAGUUTT-3'; 2) 5'-CACAUUCAAUGGAGCUGAATT-3'. After transfection of siRNA or plasmids, LX-2 cells were harvested for qPCR immunoblot or co-immunoprecipitation. Supplemental Table 1 reflects the primary sequences used for qPCR. mRNA expression was quantified by SYBR Green real-time PCR using the ABI Prism 7900 Sequence Detection System (Life Technologies, Darmstadt, Germany). Gene expression was normalized to β-actin [20, 21].

In all cases, when co-immunoprecipitation and immunoblotting were performed, the cells were washed twice in cold PBS and then lysed in immunoprecipitation (IP) lysis buffer (Pierce Co-immunoprecipitation Kit) with phosphatase and protease inhibitors [20]. Eluted proteins were separated by SDS-PAGE and thence detected by immunoblotting. Protein extraction, electrophoresis and blotting were performed as noted [1]. For visualization we used enhanced chemiluminescence [21]. The density of the immunoblots was measured by "Image J" (National Institutes of Health, MD), and normalized by GAPDH. Finally, LX-2 cells were cultured in 10cm plates and harvested for a chromatin immunoprecipitation (CHIP) assay (CHIP kit, Millipore, Danvers, MA). Briefly, we used antibody against phospho-Smad3 to bind with DNA lysed from LX-2 cells. DNA was recovered for PCR and ultimately visualized by agarose gel electrophoresis. The primer sequences for PCR reaction were as follows: forward primer, 5'-CCACCTTCCAGCCTCCAAAA-3'; reverse primer, 5'-GTTTCACCGTGTTAGCCAGG-3'.

3.1.4 Statistical analysis

All data are reported as mean ± standard error (SD). Prism 6.0 (GraphPad Software) was used to evaluate statistical differences and assessed by two-tailed unpaired Student's t-tests. A P value of less than 0.05 was considered statistically significant.

4.1 Results

4.1.1 Cthrc1 is significantly induced in murine cholestatic liver fibrosis

We first quantified changes in gene and protein expression of Cthrc1 in liver lysates in the two models of cholestatic liver fibrosis. In the CBDL model, there was a 25-fold induction of hepatic Cthrc1 mRNA 5 days after CBDL ($p<0.001$), compared to sham operated controls (Figure 1A). Immunoblotting confirmed a 7-fold ($p<0.01$) induction of Cthrc1 protein in these mice, compared to the sham group (Figure 1B). By immunohistochemical staining, the

Author Manuscript Author Manuscript Author Manuscript Author Manuscript

number of Cthrc1 positive cells per field was significantly increased ($p<0.01$) in the CBDL mice (223.60± 63.12 per field) compared with the sham group (17.60 ± 8.04 per field), and Cthrc1 was located in non-parenchymal liver cells (Figure 1C). Induction of Cthrc1 was also apparent in the DDC model. Both mRNA and protein levels of Cthrc1 were dramatically induced in the mice fed DDC-diets for 2 weeks (Figure 1D, E and F).

4.1.2 Administration of exogenous Cthrc1 has both preventive and therapeutic effects on liver fibrosis

Two weeks after the injection of adenovirus vector encoding the Cthrc1 gene (Ad-Cthrc1) or GFP (used as control, Ad-GFP), Cthrc1 mRNA in whole liver lysates was significantly increased compared to other solid organs, including heart, lung, kidney and spleen ($p<0.01$) (Figure 2A). This data was confirmed by immunoblot ($p<0.01$) (Figure 2B). There was no histologic evidence of injury in liver, brain, heart, lung, kidney, spleen, stomach or colon (data not shown).

Importantly, in Ad-Cthrc1-injected mice there was reduced liver fibrosis as assessed by Masson's trichome and picrosirius red staining (Figure 2C). A significantly decreased morphometric quantification of sirius red was noted in the Ad-Cthrc1 ($p<0.001$) treated group compared to Ad-GFP controls (Figure 2D). These findings were associated with reduced expression of profibrogenic genes including collagen type I, III and markers of HSC activation, i.e. α-SMA ($p < 0.01$) (Figure 2E). Thus, these results indicate that vector-mediated up-regulation of Cthrc1, preventing the development of hepatic fibrosis in the CBDL model. We next addressed whether the up-regulation of Cthrc1 had a therapeutic effect on ongoing hepatic fibrosis induced by CBDL. To do so, we administrated the vectors 3 days following CBDL, a time at which hepatic fibrosis had already developed; mice were studied on day 11 (Supplemental Figure 1B). First, as expected, control mice developed significant hepatic fibrosis. Importantly, the Ad-Cthrc1-treated mice demonstrated a significant reduction in fibrosis as demonstrated by Masson's trichome and picrosirius red staining (Figure 2F, arrow: fibrotic area); the morphometric quantification of sirius red was 3.70 ± 0.30% ($p<0.001$) in the Ad-GFP group compared to 1.90 ± 0.19% in Ad-Cthrc1 group (Figure 2G).

This analysis and protocol was also studied in liver fibrosis induced by feeding DDC. Vectors containing Cthrc1 or GFP genes were administrated 3 days before or 1 week after the beginning of the DDC feeding (Supplemental Figures 1C and D). In mice treated with Ad-Cthrc1 fibrosis was significantly reduced as assessed by Masson' trichome staining, sirius red staining and H&E (Figure 3A). This finding was quantified by morphometry of sirius red staining ($p<0.001$, Figure 3B) and associated with hepatic expression of profibrogenic genes, i.e. collagen type I ($P<0.01$), III ($p<0.001$), and α-SMA ($p<0.01$) (Figure 3C). In the therapeutic model, administration of Ad-Cthrc1 significantly alleviated hepatic fibrosis demonstrated by Masson' trichome staining, sirius red staining, H&E (Figure 3D), and decreased morphometric quantification of sirius red ($P<0.01$) (Figure 3E). In summary, enhanced expression of Cthrc1 not only prevented the development of cholestatic liver fibrosis, but also was therapeutic even after hepatic fibrosis had been initiated.

Author Manuscript Author Manuscript Author Manuscript Author Manuscript

4.1.3 Silencing of Cthrc1 exacerbates cholestatic liver fibrosis

Based on these data, we next determined if silencing the Cthrc1 gene in the CBDL and DDC models would exacerbate fibrosis. We used Ad-shCthrc1 containing a shRNA targeting the murine Cthrc1 gene to knock down hepatic Cthrc1. Indeed, after the administration of Ad-shCthrc1, mRNA decreased approximately 60% ($p<0.001$, Supplemental Figure 3A) compared to controls (Ad-shGFP). Of note, the kinetics of administration of the Ad-shCthrc1 injection was the same as we chose for Ad-Cthrc1 administration (Supplemental Figure 1).

Indeed, administration of Ad-shCthrc1 significantly exacerbated hepatic fibrosis induced by CBDL, when Ad-shCthrc1 was injected both before (sirius red area, $p<0.001$, Supplemental Figure 3B) and after (sirius red area, $p<0.01$, Supplemental Figure 3C) the surgery. A similar study was performed in the DDC model. Similar to CBDL, suppression of hepatic Cthrc1 by Ad-shCthrc1 exacerbated liver fibrosis both before ($p<0.01$, Supplemental Figure 4A) and after ($p < 0.05$, Supplemental Figure 4B) DDC feeding, again as reflected by trichome, picrosirius red staining and H&E. Taken together, these results further suggest that Cthrc1 acts as a negative regulator during cholestatic liver fibrosis.

4.1.4 The mechanisms of action of Cthrc1 in modulation of liver fibrosis

From our data, we noted that Cthrc1 was located in non-parenchymal cells (Figure 1C and F). Hepatic stellate cells are the most crucial non-parenchymal cells during liver fibrosis. A study reported that Cthrc1 was derived from keloid fibroblasts and colud be induced by TGF-β[22]. Hence, we speculated that HSCs might be a source of Cthrc1. To confirm this hypothesis, we assessed mRNA and protein expression of Cthrc1 in isolated rat HSCs by qPCR, immunoblot and immunofluorescence (Figure 4). During culture-activation of HSCs (cultured for 7 days *in vitro*), Cthrc1 mRNA was increased 30-fold compared to quiescent HSCs (cultured for 2 days *in vitro*) (Figure 4A). Immunoblotting confirmed this significant increase of Cthrc1 during HSC activation ($p<0.01$) (Figure 4B). Moreover, by immunofluorescence, Cthrc1 was increased during the activation of HSCs, and was predominantly expressed in cytoplasm (Figure 4C). Based on these data, we explored the mechanism of Cthrc1 on fibrosis in stellate cells. Since Cthrc1 was dramatically increased during activation of HSCs, we examined whether Cthrc1 could be induced by TGF-β1 (a key activator for HSCs). To do so, we treated LX-2 cells, a human hepatic stellate cell line with serial concentrations of TGF-β1. Cthrc1 protein was statistically induced by TGF-β1 in a dose-dependent manner, and approached a peak at 10 ng/ml compared to controls ($p<0.01$, Figure 5A). Furthermore, Cthrc1 protein was increased by TGF-β1 stimulation (5 ng/ml) in a time-dependent manner with a peak at 24 hours, approximately 25 fold compared to controls ($p<0.01$, Figure 5B). To clarify whether Cthrc1 expression in HSCs was specific for TGF-β1, another control cytokine, platelet-derived growth factor (PDGF)-BB, which also activates HSCs, was incubated with LX-2 cells. In PDGF-BB treated cells, there was no significant Cthrc1 induction (Figure 5C). These data suggest that Cthrc1 was specifically induced by TGF-β1. To confirm this result, LY2109761 (the specific inhibitors for TGF-β receptor I/II) or SB431542 [the specific inhibitors for activin receptor-like kinase 5 (ALK5), a kinase for Smad2 and Smad3] were used to block TGF-β signaling. Up-regulation of

Author Manuscript Author Manuscript Author Manuscript Author Manuscript

Cthrc1 was abolished when we blocked the TGF-β signaling pathway in HSCs ($p < 0.01$, Figure 5D and E).

TGF-β-driven Cthrc1 induction is mediated by canonical Smad signaling and inhibition of Smad3 phosphorylation abrogated induction of Cthrc1. Importantly, in silico analysis of the human promoter revealed that the phospho-Smad3 binding element is in the region −995 to −657 upstream of the transcription starting site (Figure 5F). Accordingly, a luciferase reporter carrying this promoter sequence was activated after administration of TGF-β1 (5ng/ml) (Figure 5G) or transfected with plasmid Smad3 (Figure 5H) in LX-2 cells. The luciferase reporter was activated at 12 and 24 hours after administration of TGF-β1 (Figure 5G). While Cthrc1 promoter activity was significantly increased at 24 hours ($p < 0.05$), 48 hours ($p<0.05$) and 72 hours ($p < 0.01$) after transfected with plasmid Smad3 compared to controls (Figure 5H). Chromatin immunoprecipitation (CHIP) assay was used to verify direct binding of phospho-Smad3 to the Cthrc1 promoter in LX-2 cells (Figure 5I). Thus, TGF-β induced Cthrc1 by directly recruiting phospho-Smad3 to the Cthrc1 promoter.

We next performed *in vitro* studies to confirm the mechanistic effects of Cthrc1 indicated by the murine models. Accordingly, we analyzed profibrogenic genes in LX-2 cells after transfection with Ad-Cthrc1 or controls. As expected, Cthrc1 was increased in the Ad-Cthrc1 treated LX-2 cells compared with the Ad-GFP control group (Figure 6A). TGF-β1 induced expression of collagen types I α, III, and α-SMA both in the control and Ad-Cthrc1 group. Importantly, similar to the results *in vivo*, enforced expression of Cthrc1 in LX-2 cells inhibited profibrogenic genes, including α-SMA ($p < 0.01$), collagen types I α ($p < 0.001$) and III ($p < 0.01$) induced by TGF-β1 compared to Ad-GFP controls (Figure 6B, C and D). To confirm the physiological effect of Cthrc1 in HSCs, siRNAs targeting the Cthrc1 gene were transfected to LX-2 cells. Profibrogenic genes were analyzed 48 hours later and suppression of Cthrc1 increased the expression of profibrogenic genes in LX-2 cells (Figure 6E).

4.1.5 Cthrc1 represses TGF-β signaling by accelerating degradation of phospho-Smad3

To elucidate the mechanism of Cthrc1 inhibition of profibrogenic genes induced by TGF-β1, we analyzed the phosphorylation status of Smad2 and Smad3 in LX-2 cells after transfection with Ad-Cthrc1. A schematic representation of this protocol is illustrated in Figure 7A. We treated LX-2 cells with TGF-β1 for 1 hour (5 ng/ml) to generate a pool of phospho-Smad2 and phospho-Smad3 and then added SB431542 to prevent rephosphorylation of dephosphorylated Smad2 and Smad3. These results suggested that Cthrc1 did not statistically affect the induction of phospho-smad2 and phospho-Smad3 response to TGF-β1, but promoted the disappearance of phospho-Smad3 at 1 hour ($p < 0.01$) or 2 hours ($p < 0.05$) after washout of TGF-β1, i.e. Cthrc1 accelerated the degradation of phospho-Smad3 (Figure 7B). However, the disappearance of phospho-Smad2 was not affected (Figure 7B). The proteasome pathway is known to be the key factor for degradation of phospho-Smad3 [23]. Therefore, we treated LX-2 cells with the proteosomal inhibitor MG-132 (30μM) after transfection with Ad-Cthrc1 or control. Interestingly, MG-132 abolished the accelerated degradation of phospho-Smad3 by Cthrc1 (Figure 7C). These results suggest that Cthrc1 accelerate the degradation of phospho-Smad3 via the proteosomal pathway.

Author Manuscript Author Manuscript Author Manuscript Author Manuscript

Finally, to further probe the mechanism, we examined the subcellular distribution of endogenous Cthrc1 and phospho-Smad3 in LX-2 cells and activated primary rat HSCs (cultured 7 days *in vitro*). Confocal microscopy revealed extensive overlap of Cthrc1 and phospho-Smad3 in the cytoplasm in both cells (Figure 7D and E). The interaction between endogenous Cthrc1 and phospho-smad3 was further detected by co-immunoprecipitation (Co-IP). Cthrc1 directly bound to phospho-Smad3 either in LX-2 cells or activated rat primary rat HSCs (Figure 7F). A co-immunoprecipitating assay was performed after transfection with a series of Cthrc1 truncations. The sequence between 270 bp and 357 bp was noted to be essential for the interaction between Cthrc1 and phospho-Smad3 (Figure 7G). Hence, Cthrc1 induced by TGF-β promotes the degradation of phospho-Smad3 via the proteosomal pathway, through 90-119 amino acids of Cthrc1 protein binding with phospho-Smad3, and then inhibits synthesis of profibrogenic genes in HSCs.

5.1 Discussion

We have identified Cthrc1 as a key checkpoint in cholestatic liver fibrosis. Firstly, Cthrc1 was induced at the level of both gene and protein expression following development of liver fibrosis in two murine models. Second, Cthrc1 was also induced following activation of HSCs. In addition, enhanced expression of Cthrc1 improved hepatic fibrosis induced in both models. In contrast, silencing of Cthrc1 enhanced fibrosis. We also note that administration of TGF-β1 induced Cthrc1 expression, which in turn suppressed TGF-β1 signaling to inhibit synthesis of pro-fibrogenic genes. Similarly, silencing of Cthrc1 in HSCs, promoted synthesis of pro-fibrogenic genes. TGF-β-induced Cthrc1 degrades the pool of phospho-Smad3 response to TGF-β1, which constitutes a negative feedback loop in the TGF-β pathway, consistent with the role of TGF-β1 as a central regulator of hepatic fibrosis [22, 24].

We note herein that Cthrc1 was specifically induced by TGF-β1 via phospho-Smad 3 binding with the promoter in HSCs, and then in turn accelerated degradation of phospho-Smad3. Thus, Cthrc1 and phospho-Smad3 constitute a negative feedback loop in the TGF-β pathway [25]. Negative feedback loops in the TGF-β pathway are a naturally occurring phenomena. DAP kinase-related apoptosis-inducing protein kinase 2 is induced by TGF-β, and specifically interacts with TGF-β RI, then suppresses TGF-β signaling [26]. Transmembrane prostate androgen-induced RNA and low density lipoprotein receptor class A domain containing 4 to Smad2/3 compete with the Smad anchor for receptor activation for Smad2/3 binding to attenuate recruitment of Smad2/3 to the ALK5, and suppresses TGF-β signaling [27]. We report a potentially novel negative feedback loop in the TGF-β pathway with potential therapeutic usefulness.

Sustained over-expression of the TGF-β/Smad3 pathway is a key mediator of hepatic fibrosis. Indeed, encouraging data have been obtained by blocking the TGF-β/Smad3 pathway in models of hepatic fibrosis [10], but have thus far have yielded disappointing results in humans [11]. Therapeutic dosing of a neutralizing monoclonal antibody against TGF-β1 alleviates and potentially reverses fibrosis in animal models of renal, pulmonary fibrosis and also systemic sclerosis [28–30]. Systemic administration of an anti-TGF-β1 drug in humans had no efficacy in systemic sclerosis with serious adverse events [12].

Author Manuscript Author Manuscript Author Manuscript Author Manuscript

Although overexpression of Cthrc1 may be a promising candidate for alleviating hepatic fibrosis induced by CBDL and DDC-diet feeding, there are potential adverse effects. Aberrant highly expression of Cthrc1 has been reported in solid human tumors, including melanoma [31, 32], gastric cancer [33, 34], colorectal cancer [35, 36], hepatocellular carcinoma [37, 38]. In our short term studies, overexpression of Cthrc1 did not lead to atypical pathology in brain, heart, lung, kidney, spleen, stomach and colon, consistent with reports that Cthrc1 transgenic mice do not develop tumors [39]. More importantly, Cthrc1 is a cell-type-specific inhibitor of TGF-β [15], which in turn will lead to less adverse impact on normal physiology. Notably, we found that conserved region of 90–119 amino acids in Cthrc1 protein is the motif which bind to phospho-Smad3. Therefore, the strategy of administration of Cthrc1 truncation may decrease the potential adverse effects of Cthrc1 for treating fibrosis in the future. Thus, we demonstrate that Cthrc1 is a key checkpoint that represses TGF-β signaling during cholestatic liver fibrosis. Cthrc1 is induced by TGF-β via phospho-Smad3, and then binds to phospho-Smad3, which leads to degradation via a proteosomal pathway and inhibits synthesis of HSCs profibrogenic genes (Figure 8). The potential utility of manipulating Cthrc1 to therapeutic benefit merits further exploration and is much needed [40]. Fibrosis is clearly one of the major unmet needs in liver autoimmunity and despite significant improvements in our understanding of the effector cells that lead to immunopathology, there still remains this major gap in the treatment of established fibrosis [41–50].

Supplementary Material

Refer to Web version on PubMed Central for supplementary material.

Acknowledgments

Financial Support: This work was supported by grants from the National Natural Science Foundation of China (# 81170380 and # 81325002 to Xiong Ma, # 81421001 to Jingyuan Fang, # 81400608 to Ruqi Tang, # 81200309 to Wei Zhong, # 81200293 to Qi Miao and # 81100296 to Canjie Guo); National Institutes of Health grants DK090019 (M. Eric Gershwin) and DK56621 (Scott Friedman); Doctoral Innovation Fund Projects from Shanghai Jiaotong University School of Medicine BXJ201321 (Zhaolian Bian).

Abbreviations

Cthrc1	collagen triple helix repeat containing-1
TGF-β	transforming growth factor-β
CBDL	common bile duct ligation
DDC	3, 5-diethoxycarbonyl-1, 4-dihydrocollidine
Ad	adenovirus
DMEM	dulbecco's modified eagle medium
FBS	fetal bovine serum
IB	immunoblot
ChIP	chromatin immunoprecipitation

Author Manuscript Author Manuscript Author Manuscript Author Manuscript

CO-IP	co-immunoprecipitation
ECM	extracellular matrix
HSCs	hepatic stellate cells
H&E	hematoxylin & eosin
phospho-Smad (p-Smad)	phosphorylated Smad
ALK5	activin receptor-like kinase 5
qPCR	quantitative real-time polymerase chain reaction
α-SMA	alpha smooth muscle actin

References

1. Bian Z, Peng Y, You Z, Wang Q, Miao Q, Liu Y, et al. CCN1 expression in hepatocytes contributes to macrophage infiltration in nonalcoholic fatty liver disease in mice. Journal of lipid research. 2013; 54:44–54. [PubMed: 23071295]
2. Wang Q, Selmi C, Zhou X, Qiu D, Li Z, Miao Q, et al. Epigenetic considerations and the clinical reevaluation of the overlap syndrome between primary biliary cirrhosis and autoimmune hepatitis. Journal of autoimmunity. 2013; 41:140–5. [PubMed: 23187010]
3. Friedman SL. Mechanisms of hepatic fibrogenesis. Gastroenterology. 2008; 134:1655–69. [PubMed: 18471545]
4. Francois A, Gombault A, Villeret B, Alsaleh G, Fanny M, Gasse P, et al. B cell activating factor is central to bleomycin- and IL-17-mediated experimental pulmonary fibrosis. Journal of autoimmunity. 2015; 56:1–11. [PubMed: 25441030]
5. Yao Y, Yang W, Yang YQ, Ma HD, Lu FT, Li L, et al. Distinct from its canonical effects, deletion of IL-12p40 induces cholangitis and fibrosis in interleukin-2Ralpha(−/−) mice. Journal of autoimmunity. 2014; 51:99–108. [PubMed: 24651036]
6. Lee YA, Wallace MC, Friedman SL. Pathobiology of liver fibrosis: a translational success story. Gut. 2015
7. Mederacke I, Hsu CC, Troeger JS, Huebener P, Mu X, Dapito DH, et al. Fate tracing reveals hepatic stellate cells as dominant contributors to liver fibrosis independent of its aetiology. Nature communications. 2013; 4:2823.
8. Cheng K, Yang N, Mahato RI. TGF-beta1 gene silencing for treating liver fibrosis. Molecular pharmaceutics. 2009; 6:772–9. [PubMed: 19388665]
9. Arribillaga L, Dotor J, Basagoiti M, Riezu-Boj JI, Borras-Cuesta F, Lasarte JJ, et al. Therapeutic effect of a peptide inhibitor of TGF-beta on pulmonary fibrosis. Cytokine. 2011; 53:327–33. [PubMed: 21185199]
10. Liu X, Hu H, Yin JQ. Therapeutic strategies against TGF-beta signaling pathway in hepatic fibrosis. Liver international : official journal of the International Association for the Study of the Liver. 2006; 26:8–22. [PubMed: 16420505]
11. Mehal WZ, Iredale J, Friedman SL. Scraping fibrosis: expressway to the core of fibrosis. Nature medicine. 2011; 17:552–3.
12. Denton CP, Merkel PA, Furst DE, Khanna D, Emery P, Hsu VM, et al. Recombinant human anti-transforming growth factor beta1 antibody therapy in systemic sclerosis: a multicenter, randomized, placebo-controlled phase I/II trial of CAT-192. Arthritis Rheum. 2007; 56:323–33. [PubMed: 17195236]
13. LeClair R, Lindner V. The role of collagen triple helix repeat containing 1 in injured arteries, collagen expression, and transforming growth factor beta signaling. Trends in cardiovascular medicine. 2007; 17:202–5. [PubMed: 17662915]

Author Manuscript Author Manuscript Author Manuscript Author Manuscript

14. Pyagay P, Heroult M, Wang Q, Lehnert W, Belden J, Liaw L, et al. Collagen triple helix repeat containing 1, a novel secreted protein in injured and diseased arteries, inhibits collagen expression and promotes cell migration. Circulation research. 2005; 96:261–8. [PubMed: 15618538]
15. LeClair RJ, Durmus T, Wang Q, Pyagay P, Terzic A, Lindner V. Cthrc1 is a novel inhibitor of transforming growth factor-beta signaling and neointimal lesion formation. Circulation research. 2007; 100:826–33. [PubMed: 17322174]
16. Zhang H, Liu Y, Bian Z, Huang S, Han X, You Z, et al. The critical role of myeloid-derived suppressor cells and FXR activation in immune-mediated liver injury. Journal of autoimmunity. 2014 Epub ahead of print.
17. Zhong W, Shen WF, Ning BF, Hu PF, Lin Y, Yue HY, et al. Inhibition of extracellular signal-regulated kinase 1 by adenovirus mediated small interfering RNA attenuates hepatic fibrosis in rats. Hepatology. 2009; 50:1524–36. [PubMed: 19787807]
18. Guo CJ, Pan Q, Li DG, Sun H, Liu BW. miR-15b and miR-16 are implicated in activation of the rat hepatic stellate cell: An essential role for apoptosis. Journal of hepatology. 2009; 50:766–78. [PubMed: 19232449]
19. Nipic D, Pirc A, Banic B, Suput D, Milisav I. Preapoptotic cell stress response of primary hepatocytes. Hepatology. 2010; 51:2140–51. [PubMed: 20513000]
20. Kong X, Qian J, Chen LS, Wang YC, Wang JL, Chen H, et al. Synbindin in extracellular signal-regulated protein kinase spatial regulation and gastric cancer aggressiveness. Journal of the National Cancer Institute. 2013; 105:1738–49. [PubMed: 24104608]
21. Tang Y, Bian Z, Zhao L, Liu Y, Liang S, Wang Q, et al. Interleukin-17 exacerbates hepatic steatosis and inflammation in non-alcoholic fatty liver disease. Clinical and experimental immunology. 2011; 166:281–90. [PubMed: 21985374]
22. Li J, Cao J, Li M, Yu Y, Yang Y, Xiao X, et al. Collagen triple helix repeat containing-1 inhibits transforming growth factor-β1-induced collagen type I expression in keloid. British Journal of Dermatology. 2011; 164:1030–6. [PubMed: 21667528]
23. Lin X, Duan X, Liang YY, Su Y, Wrighton KH, Long J, et al. PPM1A functions as a Smad phosphatase to terminate TGFbeta signaling. Cell. 2006; 125:915–28. [PubMed: 16751101]
24. Palumbo-Zerr K, Zerr P, Distler A, Fliehr J, Mancuso R, Huang J, et al. Orphan nuclear receptor NR4A1 regulates transforming growth factor-beta signaling and fibrosis. Nature medicine. 2015; 21:150–8.
25. Deng YR, Ma HD, Tsuneyama K, Yang W, Wang YH, Lu FT, et al. STAT3-mediated attenuation of CCl4-induced mouse liver fibrosis by the protein kinase inhibitor sorafenib. Journal of autoimmunity. 2013; 46:25–34. [PubMed: 23948302]
26. Yang K-M, Kim W, Bae E, Gim J, Weist Brian M, Jung Y, et al. DRAK2 Participates in a Negative Feedback Loop to Control TGF-β/Smads Signaling by Binding to Type I TGF-β Receptor. Cell Reports. 2012; 2:1286–99. [PubMed: 23122956]
27. Nakano N, Maeyama K, Sakata N, Itoh F, Akatsu R, Nakata M, et al. C18 ORF1, a novel negative regulator of transforming growth factor-beta signaling. The Journal of biological chemistry. 2014; 289:12680–92. [PubMed: 24627487]
28. McCormick LL, Zhang Y, Tootell E, Gilliam AC. Anti-TGF-beta treatment prevents skin and lung fibrosis in murine sclerodermatous graft-versus-host disease: a model for human scleroderma. Journal of immunology. 1999; 163:5693–9.
29. Ling H, Roux E, Hempel D, Tao J, Smith M, Lonning S, et al. Transforming growth factor beta neutralization ameliorates pre-existing hepatic fibrosis and reduces cholangiocarcinoma in thioacetamide-treated rats. PloS one. 2013; 8:e54499. [PubMed: 23349909]
30. Ikawa Y, Ng PS, Endo K, Kondo M, Chujo S, Ishida W, et al. Neutralizing monoclonal antibody to human connective tissue growth factor ameliorates transforming growth factor-beta-induced mouse fibrosis. Journal of cellular physiology. 2008; 216:680–7. [PubMed: 18481257]
31. Li J, Zhang Z, Li G. Patient outcome prediction using multiple biomarkers in human melanoma: A clinicopathological study of 118 cases. Experimental and therapeutic medicine. 2011; 2:131–5. [PubMed: 22977480]

Author Manuscript Author Manuscript Author Manuscript Author Manuscript

32. Tang L, Dai DL, Su M, Martinka M, Li G, Zhou Y. Aberrant expression of collagen triple helix repeat containing 1 in human solid cancers. Clinical cancer research : an official journal of the American Association for Cancer Research. 2006; 12:3716–22. [PubMed: 16778098]
33. Gu L, Liu L, Zhong L, Bai Y, Sui H, Wei X, et al. Cthrc1 overexpression is an independent prognostic marker in gastric cancer. Human pathology. 2014; 45:1031–8. [PubMed: 24746208]
34. Wang P, Wang YC, Chen XY, Shen ZY, Cao H, Zhang YJ, et al. CTHRC1 is upregulated by promoter demethylation and transforming growth factor-beta1 and may be associated with metastasis in human gastric cancer. Cancer science. 2012; 103:1327–33. [PubMed: 22590977]
35. Tan F, Liu F, Liu H, Hu Y, Liu D, Li G. CTHRC1 is associated with peritoneal carcinomatosis in colorectal cancer: a new predictor for prognosis. Medical oncology. 2013; 30:473. [PubMed: 23359115]
36. Palma M, Lopez L, Garcia M, de Roja N, Ruiz T, Garcia J, et al. Detection of collagen triple helix repeat containing-1 and nuclear factor (erythroid-derived 2)-like 3 in colorectal cancer. BMC clinical pathology. 2012; 12:1–12. [PubMed: 22240170]
37. Yu-Ling Chen T-HW, Hsu Hey-Chi, Yuan Ray-Hwang, Jeng Yung-Ming. Overexpression of CTHRC1 in Hepatocellular Carcinoma Promotes Tumor Invasion and Predicts Poor Prognosis. PloS one. 2013; 8:e70324. [PubMed: 23922981]
38. Tameda M, Sugimoto K, Shiraki K, Yamamoto N, Okamoto R, Usui M, et al. Collagen triple helix repeat containing 1 is overexpressed in hepatocellular carcinoma and promotes cell proliferation and motility. International journal of oncology. 2014; 45:541–8. [PubMed: 24841500]
39. Kimura H, Kwan KM, Zhang Z, Deng JM, Darnay BG, Behringer RR, et al. Cthrc1 is a positive regulator of osteoblastic bone formation. PloS one. 2008; 3:e3174. [PubMed: 18779865]
40. Hintermann E, Ehser J, Bayer M, Pfeilschifter JM, Christen U. Mechanism of autoimmune hepatic fibrogenesis induced by an adenovirus encoding the human liver autoantigen cytochrome P450 2D6. Journal of autoimmunity. 2013; 44:49–60. [PubMed: 23809878]
41. Beuers U, Gershwin ME. Unmet challenges in immune-mediated hepatobiliary diseases. Clinical reviews in allergy & immunology. 2015; 48:127–31. [PubMed: 25820618]
42. Floreani A, Franceschet I, Perini L, Cazzagon N, Gershwin ME, Bowlus CL. New therapies for primary biliary cirrhosis. Clinical reviews in allergy & immunology. 2015; 48:263–72. [PubMed: 25331740]
43. Gershwin ME, Mackay IR, Sturgess A, Coppel RL. Identification and specificity of a cDNA encoding the 70 kd mitochondrial antigen recognized in primary biliary cirrhosis. Journal of immunology. 1987; 138:3525–31.
44. Li Y, Wang W, Tang L, He X, Yan X, Zhang X, et al. Chemokine (C-X-C motif) ligand 13 promotes intrahepatic chemokine (C-X-C motif) receptor 5+ lymphocyte homing and aberrant B-cell immune responses in primary biliary cirrhosis. Hepatology. 2015; 61:1998–2007. [PubMed: 25627620]
45. Wallach-Dayan SB, Elkayam L, Golan-Gerstl R, Konikov J, Zisman P, Dayan MR, et al. Cutting edge: FasL(+) immune cells promote resolution of fibrosis. Journal of autoimmunity. 2015; 59:67–76. [PubMed: 25812467]
46. Wang L, Sun Y, Zhang Z, Jia Y, Zou Z, Ding J, et al. CXCR5+ CD4+ T follicular helper cells participate in the pathogenesis of primary biliary cirrhosis. Hepatology. 2015; 61:627–38. [PubMed: 25042122]
47. Zhang J, Zhang W, Leung PS, Bowlus CL, Dhaliwal S, Coppel RL, et al. Ongoing activation of autoantigen-specific B cells in primary biliary cirrhosis. Hepatology. 2014; 60:1708–16. [PubMed: 25043065]
48. Lleo A, Zhang W, McDonald WH, Seeley EH, Leung PS, Coppel RL, et al. Shotgun proteomics: identification of unique protein profiles of apoptotic bodies from biliary epithelial cells. Hepatology. 2014; 60:1314–23. [PubMed: 24841946]
49. Gershwin ME, Krawitt EL. Autoimmune hepatitis: 50 Years of (slow) progress. Hepatology. 2014; 59:754–6. [PubMed: 24712041]
50. Yang CY, Ma X, Tsuneyama K, Huang S, Takahashi T, Chalasani NP, et al. IL-12/Th1 and IL-23/Th17 biliary microenvironment in primary biliary cirrhosis: implications for therapy. Hepatology. 2014; 59:1944–53. [PubMed: 24375552]

Author Manuscript Author Manuscript Author Manuscript Author Manuscript

Highlights

- A major unmet need in autoimmunity and cholestatic liver disease is the prevention and treatment of fibrosis.
- Knocking in/knockout out the Cthrc1 gene significantly modulates cholestatic fibrosis in two murine models.
- The mechanism of Cthrc1 gene expression and its effect on fibrosis is by TGF-β1 via phospho-Smad3 binding.
- Cthrc1 inhibits TGF-β signaling through a proteosomal pathway.
- Use of truncated fragments of Cthrc1 may reduce potential toxicity and serve as a model to not only further understand fibrosis, but also as a therapeutic tool.

Author Manuscript Author Manuscript Author Manuscript Author Manuscript

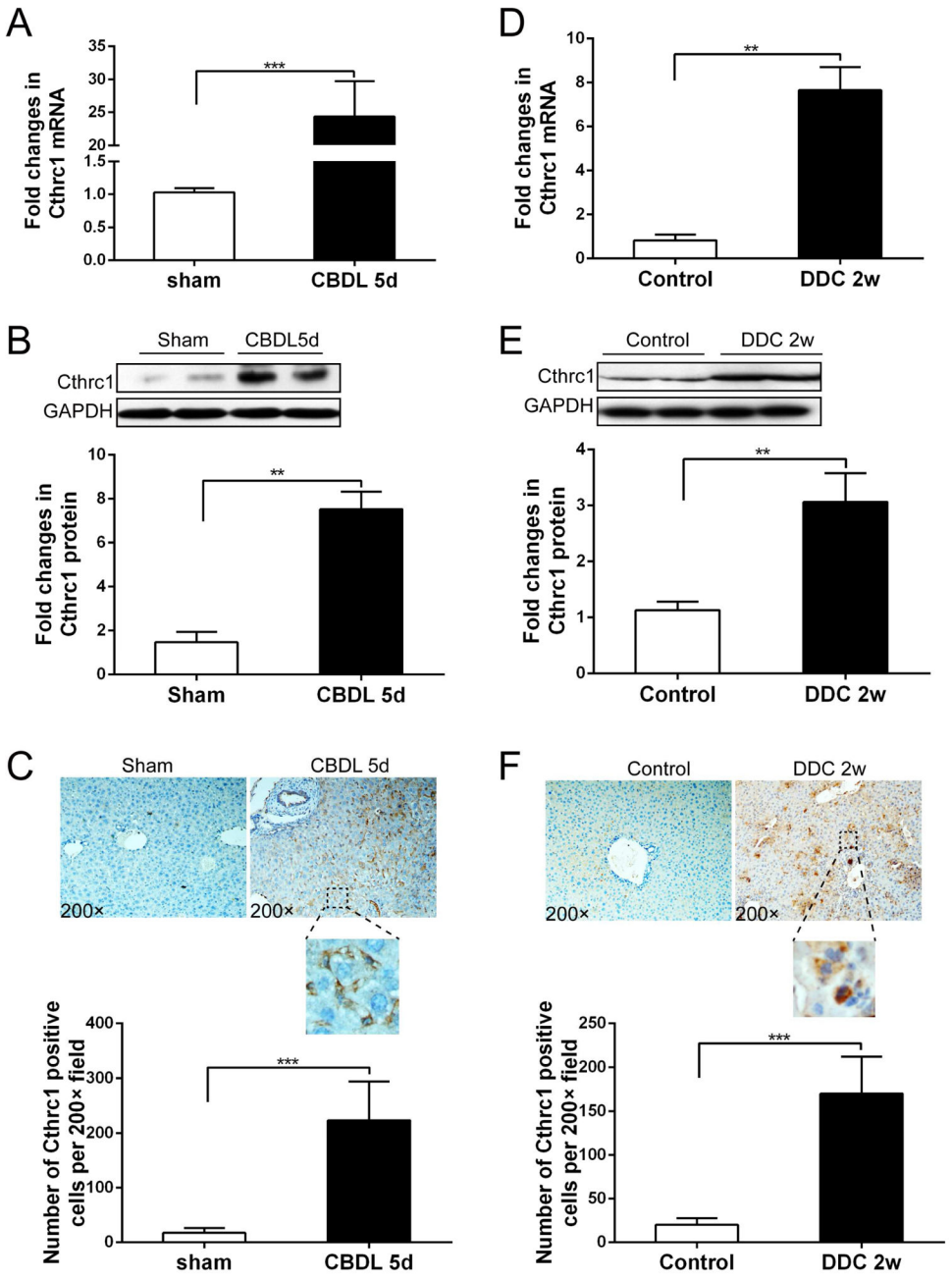

Figure 1.

Cthrc1 was incresased in murine cholestatic liver fibrosis. (A) Hepatic Cthrc1 mRNA detected by qPCR was increased in mice following CBDL compared with the sham group. (B) Immunoblotting of hepatic Cthrc1 shown its protein was induced in the CBDL group. The Image J software quantified Cthrc1 bands are normalized to their respective GAPDH and represented as fold change. (C) Representative images of hepatic immunohistochemical staining of Cthrc1 in the CBDL and sham group. The number of Cthrc1 possitive cells was dramatically increased in CBDL group compared with sham. The score of Cthrc1 possitive cells was based on image analysis of at least five random fields. (D) qPCR was used to

Author Manuscript Author Manuscript Author Manuscript Author Manuscript

detect hepatic Cthrc1 mRNA in mice fed DDC for 2 weeks or control. (E) Immunoblotting of hepatic Cthrc1 in mice fed DDC for 2 weeks or control. The Image J software quantified Cthrc1 bands are normalized to their respective GAPDH and represented as fold change. (F) Representative images of hepatic immunohistochemical staining of Cthrc1 in mice fed DDC for 2 weeks or control. The number of Cthrc1 positive cells was used for statistical analysis. (n=5 in each group, ** $p < 0.01$; *** $p < 0.001$).

Author Manuscript Author Manuscript Author Manuscript Author Manuscript

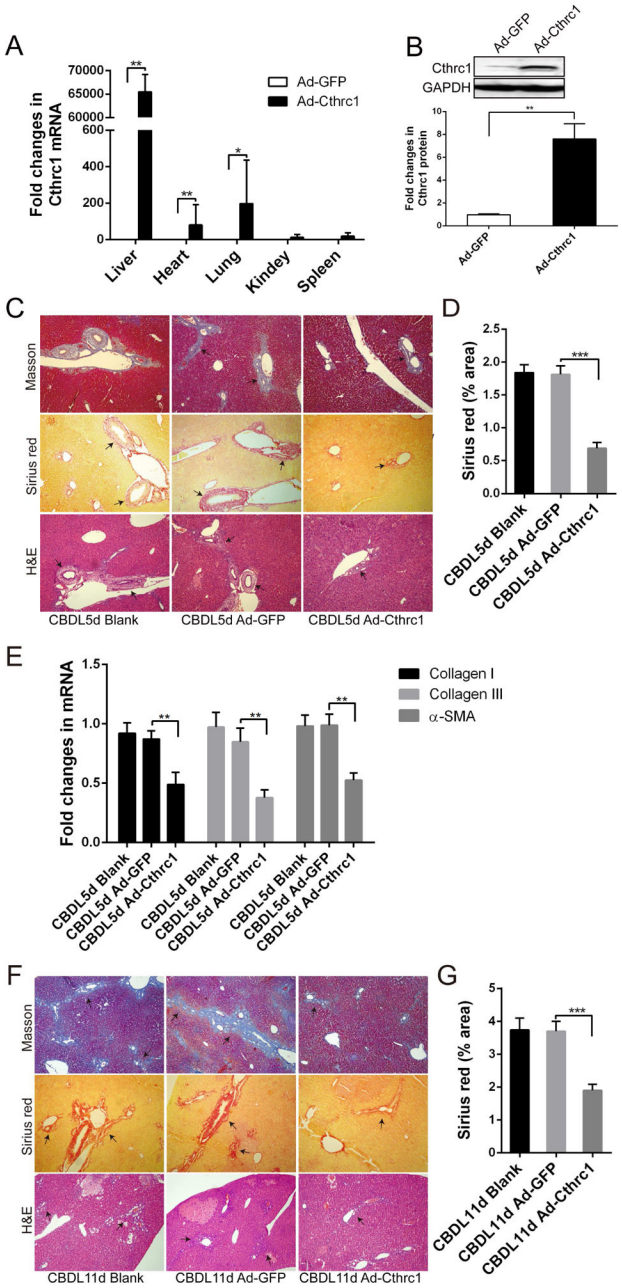

Figure 2.

Cthrc1 attenuates liver fibrosis induced by CBDL. (A) Cthrc1 mRNA was dramatically increased in liver compared with heart, lung, kidney and spleen in mice injected with Ad-Cthrc1 for 2 weeks (n=3 in each group). (B) Immunoblot analysis of hepatic Cthrc1 in mice injected with Ad-Cthrc1 and Ad-GFP. The Image J software quantified Cthrc1 bands are normalized to their respective GAPDH and represented as fold change of Ad-GFP group. (n=3 in each group). (C) Masson's trichome (top, arrow: fibrotic area), picrosirius red staining (middle, arrow: fibrotic area) and H&E (bottom, arrow: fibrotic area), of liver tissue from Ad-GFP (n=8) and Ad-Cthrc1 (n=8) injected mice, 5 days after CBDL (magnification

Author Manuscript Author Manuscript Author Manuscript Author Manuscript

100×). (D) Graph is quantification of sirius red stained areas based on image analysis of at least five random fields in each slide in the preventative CBDL model. (E) qPCR of collagen types I α, III and α-SMA in the preventative CBDL model and represented as fold change of CBDL 5d blank group. (F) Masson's trichome (top, arrow: fibrotic area), picrosirius red staining (middle, arrow: fibrotic area) and H&E (bottom, arrow: fibrotic area) of liver tissue in the therapeutic CBDL model (n = 5 in each group). (G) Graph is quantification of sirius red stained areas based on image analysis of at least five random fields in each slide in the therapeutic CBDL model. (* $p < 0.05$; ** $p < 0.01$, *** $p < 0.001$).

Author Manuscript Author Manuscript Author Manuscript Author Manuscript

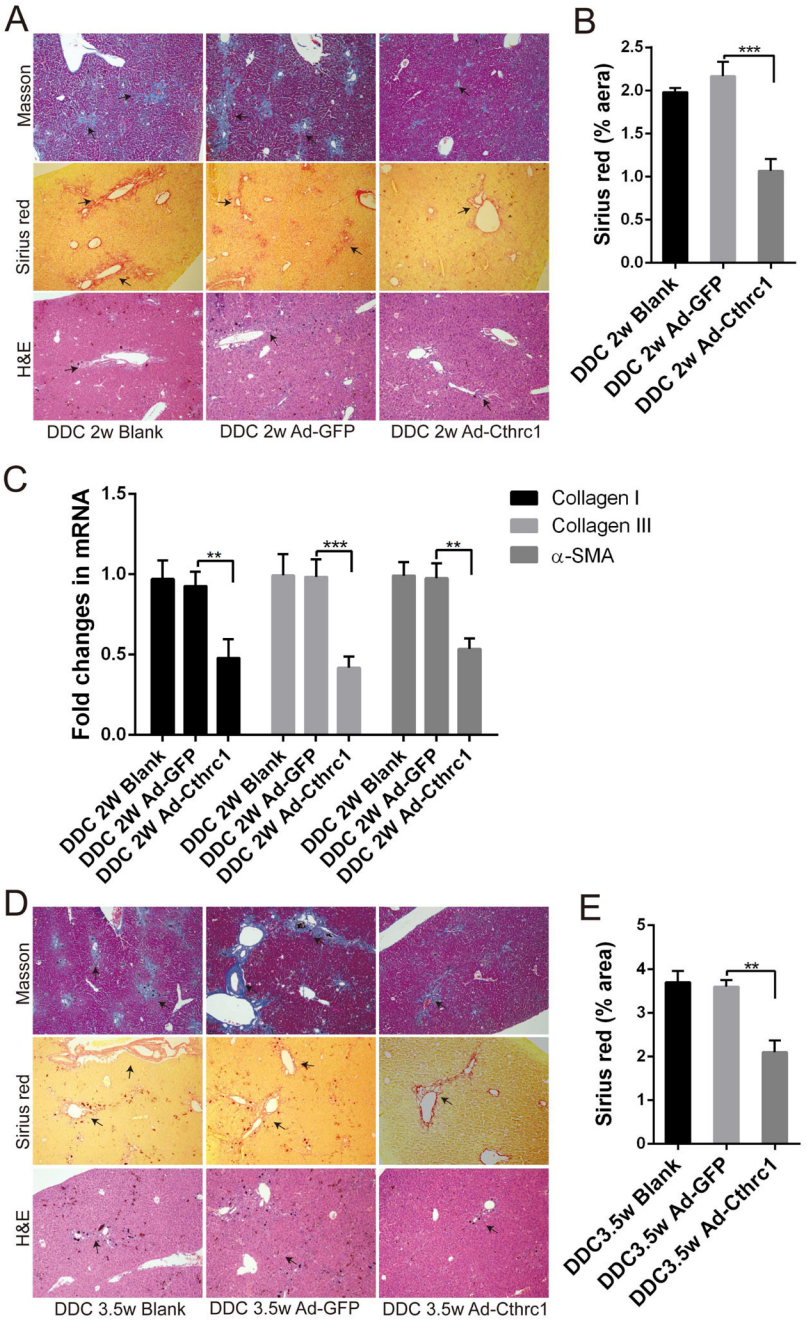

Figure 3.

Enhanced expression of hepatic Cthrc1 alleviates cholestatic liver fibrosis in mice fed DDC. (A) Masson's trichome (top, arrow: fibrotic area), picrosirius red staining (middle, arrow: fibrotic area) and H&E (bottom, arrow: fibrotic area) of liver from untreated (n=5), Ad-GFP (n=6) or Ad-Cthrc1 (n=6) injected mice following 2 weeks of the DDC-diet (magnification 100×). (B) Graph is quantification of sirius red stained areas based on image analysis of at least five random fields in each slide in the preventative DDC model. (C) Hepatic qPCR of collagen types I α , III and α-SMA in the preventative DDC model and represented as fold

Author Manuscript Author Manuscript Author Manuscript Author Manuscript

change of DDC 2w blank group. (D) Masson's trichome (top, arrow: fibrotic area), picrosirius red staining (middle, arrow: fibrotic area) and H&E (bottom, arrow: fibrotic area) in the therapeutic DDC model in untreated (n=5), Ad-GFP (n=6) or Ad-Cthrc1 (n=8) injected mice (magnification 100×). (E) Graph is quantification of sirius red stained areas based on image analysis of at least five random field in each slides in the therapeutic DDC model. (** $p < 0.01$, *** $p < 0.001$).

Author Manuscript Author Manuscript Author Manuscript Author Manuscript

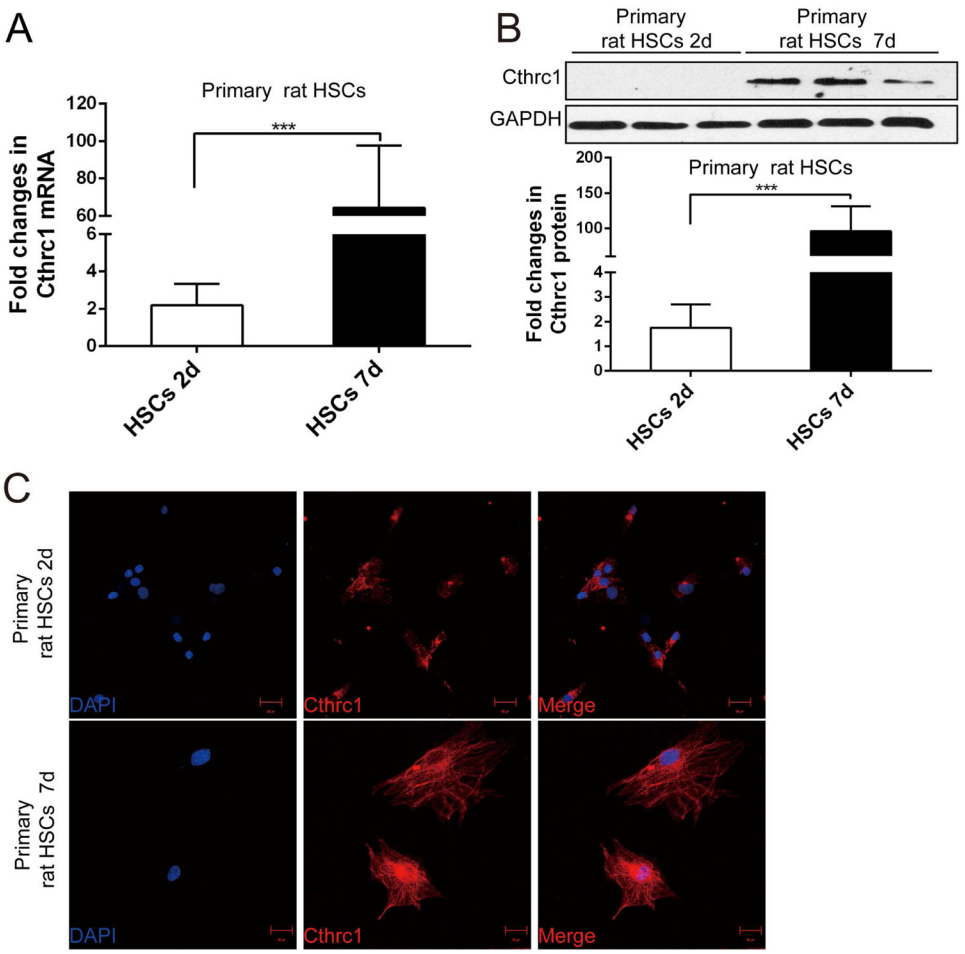

Figure 4.

Activation of HSCs increases expression of Cthrc1. (A) Cthrc1 mRNA was increased following the activation of primary rat HSCs and represented as fold change of HSCs 2d. The experiments were repeated for three times. (B) Immunoblotting of Cthrc1 in activated rat HSCs (7d, cultured for 7days *in vitro*) compared with quiescent HSCs (2d, cultured for 2days *in vitro*). The Image J software quantified Cthrc1 bands are normalized to their respective GAPDH and represented as fold change of quiescent HSCs. (C) Immunofluorescence of Cthrc1 in quiescent rat HSCs (primary rat HSCs 2d) and activated rat HSCs (primary rat HSCs 7d). Note that Cthrc1 was stained red and the cell nucleus stained with 4, 6-diamidino-2-phenylindole (DAPI) in blue, scale bars indicate 10μm. (*** $p < 0.001$)

Author Manuscript Author Manuscript Author Manuscript Author Manuscript

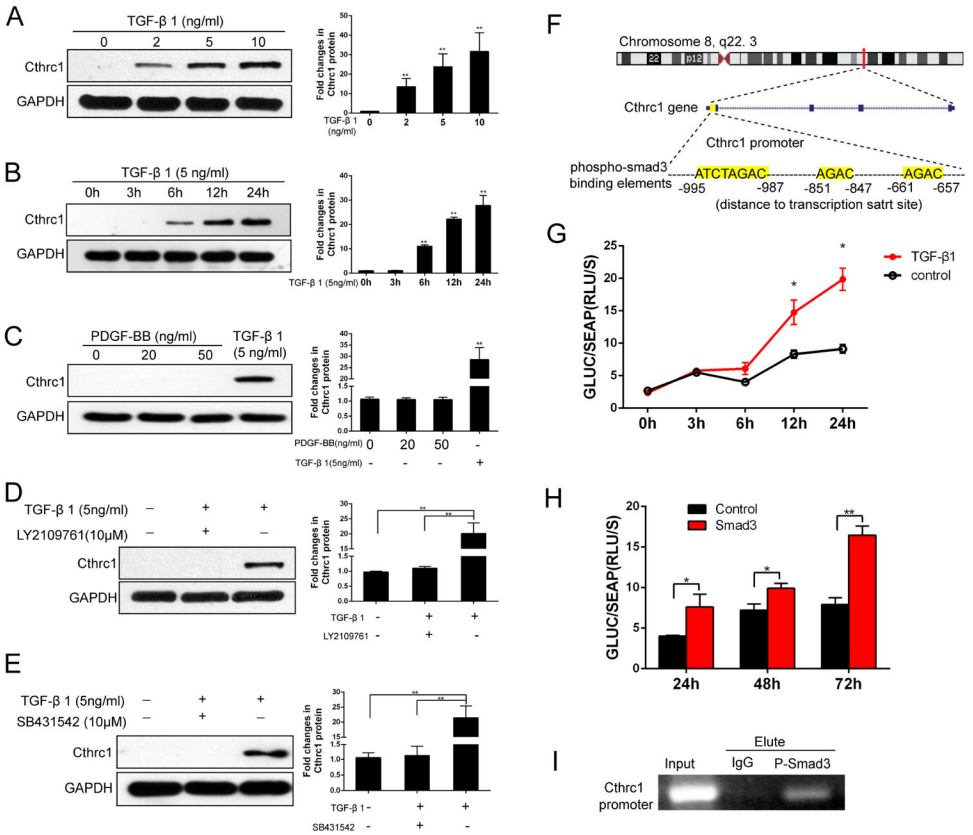

Figure 5.

Induction of Cthrc1 by TGF-β signaling. (A) Immunoblotting of starved LX-2 cells treated with serial concentrations of TGF-β1 for 24 hours. (B) Kinetics of Cthrc1 up-regulation induced by TGF-β1(5ng/ml). (C) Immunoblotting of starved LX-2 cells following treatment with PDGF-BB or TGF-β 1 for 24 hours. (D, E) Immunoblot analysis of starved LX-2 cells pretreated with LY2109761(10μM) or SB431542(10μM) for 1 hour followed by stimulation with TGF-β1(5ng/ml) for 24 hours. The Image J software quantified Cthrc1 bands are normalized to their respective GAPDH and represented as fold change. (F) Localization of the phospho-smad3 binding elements on the Cthrc1 promoter. The Cthrc1 gene promoter contains multiple binding elements for phospho-smad3 (highlighted in yellow) in the region between -995 and -657 base pairs upstream of the transcription start site. This DNA sequence was inserted into the luciferase reporter to test the transactivity of phospho-smad3 to Cthrc1. (G) A luciferase reporter assay carrying the Cthrc1 promoter sequence was transfected in LX-2 cells, and thence treated with or without TGF-β1(5ng/ml) at the indicated times. The luciferase activity was quantified as the ratio of GLU/SEAP. (H) A luciferase reporter assay carrying Cthrc1 promoter sequence and plasmid Smad3 or control plasmid were co-transfected in LX-2 cells, thence luciferase was quantified as the ratio of GLU/SEAP. (I) Chromatin immunoprecipitation (ChIP) demonstrated binding of phospho-smad3 to the Cthrc1 promoter. The input DNA and ChIP yield using nonspecific immunoglobulin G (IgG) are utilized as controls. (*$p < 0.05$; ** $p < 0.01$)

Author Manuscript Author Manuscript Author Manuscript Author Manuscript

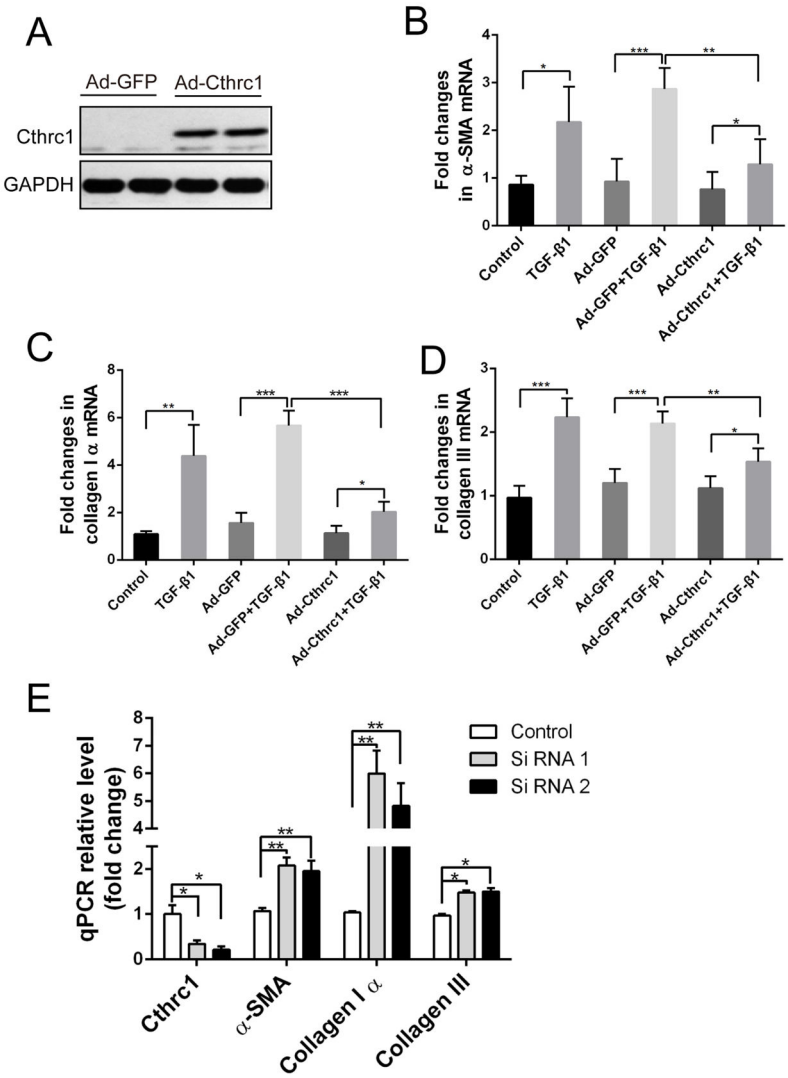

Figure 6.

Cthrc1 suppresses TGF-β signaling. (A) Immunoblot analysis of LX-2 cells transfected with Ad-Cthrc1 for 72h. (B, C, D) Enhanced expression of Cthrc1 inhibits synthesis of α-SMA, collagen types I α and III induced by TGF-β1 in LX-2 cells. The results are represented as fold change of controls. (E) Detection by qPCR of Cthrc1, α-SMA, collagen types I α and III mRNA in LX-2 cells after transfection with the siRNAs targeting Cthrc1 gene or control siRNA for 48 hours. (*p<0.05; ** p< 0.01, *** p<0.001)

Author Manuscript Author Manuscript Author Manuscript Author Manuscript

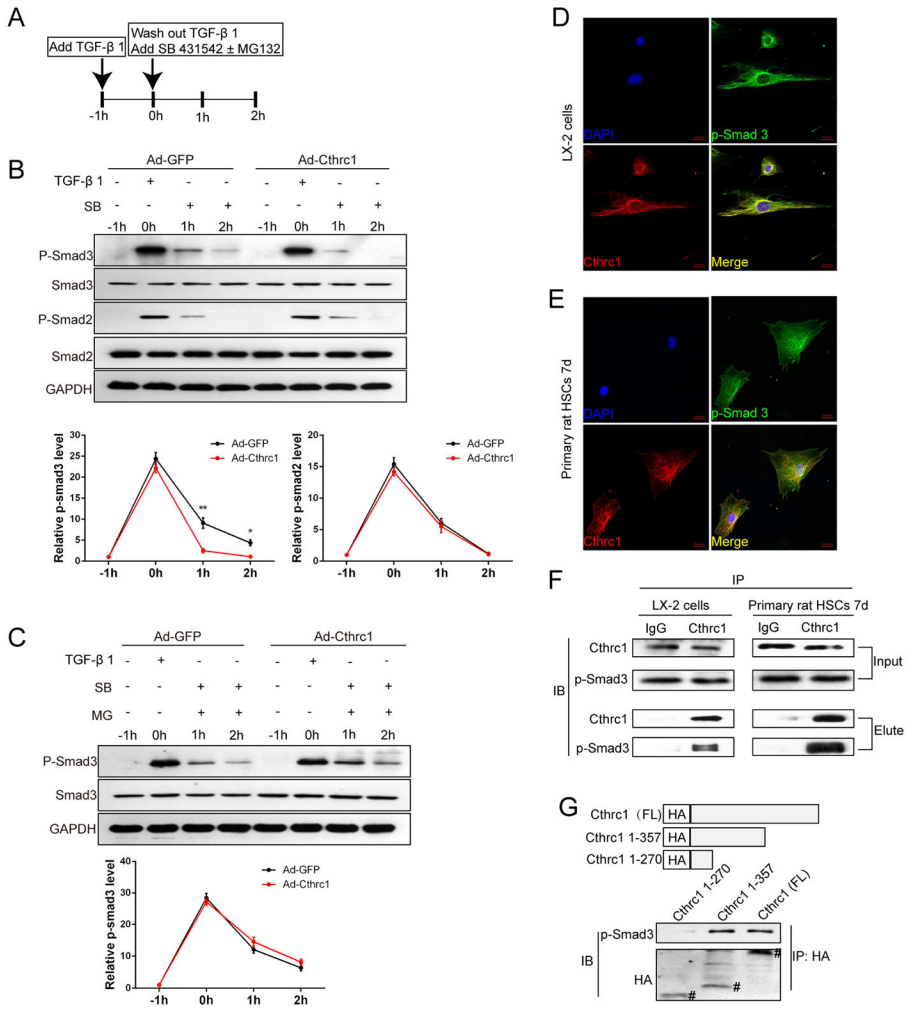

Figure 7.

Cthrc1 promote degradation of phospho-Smad3 induced by TGF-β1. (A) A schematic protocol is illustrated for B and C. (B) Immunoblotting of phospho-Smad2 and phospho-Smad3 responses to TGF-β 1 in LX-2 cells after transfection with Ad-Cthrc1 for 72 hours. Relative phospho-Smad2 (over total Smad2) and phospho-Smad3 (over total Smad3) from 3 independent experiments. (TGF-β1, 5 ng/ml; SB431542, 10 μM). (C) Immunoblotting of phospho-Smad3 in LX-2 cells after transfection with Ad-Cthrc1 or control and pretreatment with or without MG132 (30 μM). Relative phospho-Smad3 (over total Smad3) from 3 independent experiments (SB431542, 10 μM). (D, E) Immunofluorescent staining of endogenous Cthrc1 and phospho-Smad3 in LX-2 cells and activated primary rat HSCs (cultured for 7 days *in vitro*) (red, Cthrc1; green, phospho-smad3; blue, nucleus). Scale bars indicate 20μm. (F) Co-immunoprecipitation of endogenous Cthrc1 and phospho-Smad3 in LX-2 cells and activated primary rat HSCs (cultured for 7 days *in vitro*). IgG was used as a negative control. (G) Top 3 rows: plasmids containing HA-fused full-length (FL) or truncated Cthrc1 CDS regions are shown. Bottom, co-immunoprecipitation assays after transfection with plasmids containing HA-fused full-length or truncated Cthrc1 CDS

regions. (#, HA immunoblot, protein recovered from the co-immunoprecipitation complex). IP, immunoprecipitation; IB, immunoblot. (*$p<0.05$; ** $p<0.01$).

Author Manuscript Author Manuscript Author Manuscript Author Manuscript

Author Manuscript Author Manuscript Author Manuscript Author Manuscript

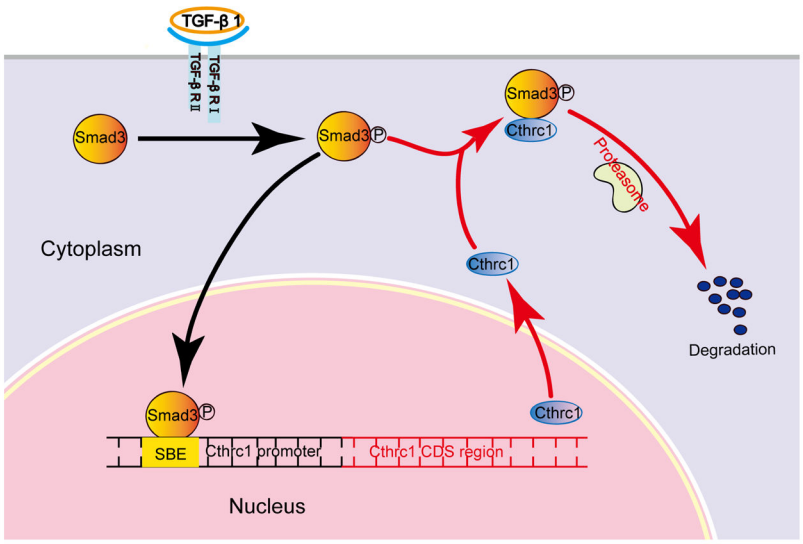

Figure 8.

Schematic representation of the proposed mechanism of Cthrc1 suppression of TGF-β signaling. Cthrc1 is induced by the TGF-β1/phospho-Smad3 signaling pathway, and thence accelerates degradation of phospho-Smad3 via proteasome pathway, thus forming a negative feedback loop, which inhibits synthesis of pro-fibrotic genes.